Supplement of Atmos. Chem. Phys., 16, 12849–12859, 2016
http://www.atmos-chem-phys.net/16/12849/2016/
doi:10.5194/acp-16-12849-2016-supplement

Supplement of

Emissions of carbon tetrachloride from Europe

Francesco Graziosi et al.

Correspondence to: Michela Maione (michela.maione@uniurb.it)

Dispersion model

We run the Lagrangian particle dispersion model FLEXPART v-9.02 (Stohl et al., 1998, 2005; http://www.flexpart.eu) releasing every three hours, from all measurement sites, 40 000 particles followed backward in time for 20 days. This in order to calculate the emission sensitivity footprint also called source-receptor-relationship (SRR). The SRR describes the relationship between the contribution of potential sources at the receptor and the change in mixing ratios at the measurement site. Fig. S1 shows the SRR for the three single stations, highlighting how the two continental stations (CMN and JFJ) are influenced by air masses originating in central Europe, whereas MHD is predominately influenced by Atlantic/Arctic air masses.

Fig. S2 shows the yearly (2012) emissions sensitivity produced using the three measurement sites. We observe a good SRR in the whole European Geographic Domain (EGD), with the exception of a small region in the Aegean area.

All the simulations are driven by European Centre for Medium-range Weather Forecast wind fields using 3-hourly ERA-Interim reanalyses (analysis fields at 00:00, 06:00, 12:00 and 18:00 UTC, and 3-h forecasts at 03:00, 09:00, 15:00 and 21:00 UTC were used) with 1°x1° horizontal resolution and 91 vertical levels.

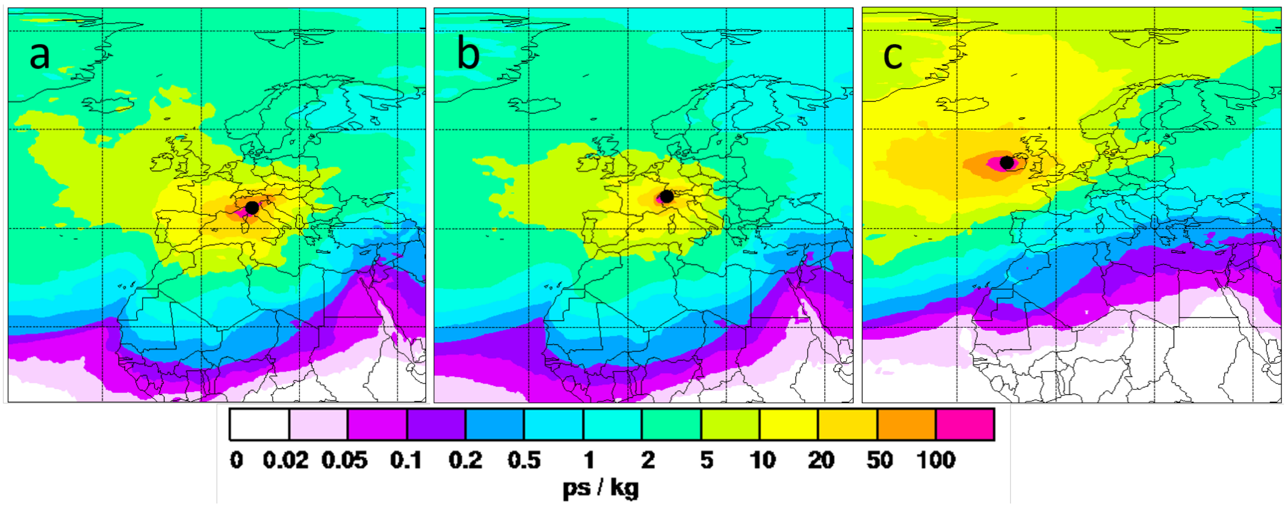

Figure S1. Single station SRR maps expressed in picoseconds per kilogram (ps kg^{-1}) obtained from FLEXPART 20 days backward calculations averaged over year 2012. Measurement sites are marked with black dots.

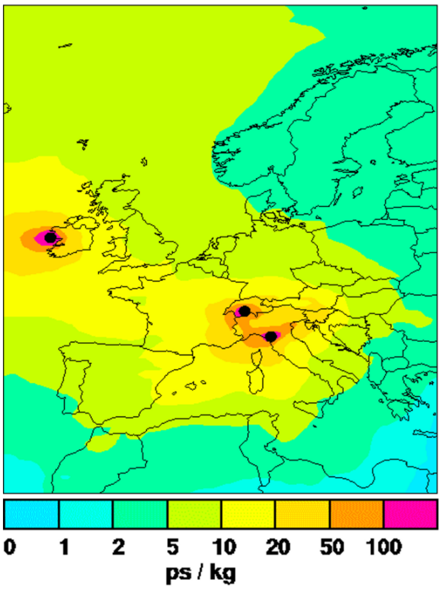

Figure S2. As in Figure S1, but for the three stations.

Inversion method

To estimate the emissions of CCl_4 from the EGD we used the inversion method, based on a Bayesian optimization technique, described by Stohl et al. (2009, 2010), where all mathematical details can be found. The emission distribution and intensity found by the inversion represent the best fit between observation data and model simulation. Using a limited number of stations not all regions are well constrained by the observations, making the problem ill-conditioned and unstable. Therefore, to get the solution to our problem, we used an a priori gridded field of emission distribution and the associated uncertainty (Stohl et al., 2009; 2010).
The cost function to be minimized is:

$$1)\ \ J = (M\tilde{x} - \tilde{y})^T diag({\sigma_0}^{-2})(M\check{x} - \tilde{y}) + \tilde{x}^T diag({\sigma_x}^{-2})\tilde{x}$$

Where the matrix *M* contains the model sensitivity, in our case all simulations produced by 40.000 particles run in backward mode for 20 days; the term $\tilde{x}$ represents the difference between the *a posteriori* and *a priori* emission vectors; $\tilde{y}$ is the difference between the observations and *a priori* simulated mixing ratios, ${\sigma_0}^{-2}$ is the vector of the standard error of observations, and ${\sigma_x}^{-2}$ is the *a priori* standard error vector.
Overall, the Bayesian inversion minimizes the cost-function reducing the model-observation misfit, represented by the first term on the right side of equation 1, optimizing the deviation of the solution from *a priori* emissions and its uncertainty, expressed by the second term of equation 1.

Uncertainty evaluation

We associate for every grid cell an uncertainty value, σ_x^j

$$2)\quad \sigma^{j}_{x\_priori} = p * \max\,(k * x_j; l * x_{surf})$$

Where p is an appropriate uncertainty scaling factor; x_j the *a priori* emission value in grid j; x_{surf} the average land surface emissions flux; k and l are scaling factors set at 0.5 and 1, respectively (Keller et al., 2011; Fang et al., 2014; Maione et al., 2014). The last term on the right side of equation 2 allows associating large uncertainty values even to low emission grid cells. We tested several uncertainty scaling factors p in order to optimise the agreement between modelled and observed mixing ratios. The increase of the uncertainty scaling factor p yields a higher variability of the *a posteriori* flux from the single grid cells, leading to a decreasing root mean square (RMS) and increasing correlation coefficients between modelled and observed mixing ratios in all the three stations. However, for p values larger than 6, new hotspots emerge in the *a posteriori* emission field with unrealistically large emissions from low sensitivity regions. We used p = 2, a value giving higher correlation coefficients and lower RMS values. Noteworthy, differences in the EGD emissions lower than 5 % are obtained using p values ranging between 1.5 and 4. The minimisation of the cost function reduces the *a priori* sigma value $\sigma^{j}_{x\_priori}$ giving, for each inverted grid cell an uncertainty value $\sigma^{j}_{x\_posteriori}$. For the whole domain we obtained an average uncertainty $\sigma^{j}_{x\_posteriori} \cong 33\%$, with a smaller uncertainty (≈20 %) in high sensitivity boxes close to the receptors (e.g., FR and UK) and a larger uncertainty (≈80 %) in low sensitivity regions far away from the receptors (e.g., Scandinavian region).

E-PRTR and Eurochlor

The *a priori* emission field used in this study makes use of the European Pollutant Release and Transfer Register (E-PRTR) (http://prtr.ec.europa.eu/) inventory and of the Eurochlor reports (http://www.eurochlor.org/).

E-PRTR

E-PRTR is the Europe-wide register that provides data from industrial facilities in European Union Member States and in Iceland, Liechtenstein, Norway, Serbia and Switzerland. It replaced and improved upon the previous European Pollutant Emission Register (EPER). The register contains data reported annually by more than *30,000 industrial facilities* covering 65 economic activities across Europe. For each facility, information are provided concerning the amounts of pollutant releases to air, water and land as well as off-site transfers of waste and of pollutants in wastewater from a list of 91 key pollutants including CCl_4. Over the period 2007-2014, 37 CCl_4 emitting activities are reported. According to E-PRTR, the “industrial scale production of basic organic chemical” is the main CCl_4 declared source in the database, being responsible for the 93.9 % of total European emissions, as shown in Figure S3 reporting the percentage contribution to CCl_4 emissions from each industrial facility, averaged over 2007-2014.

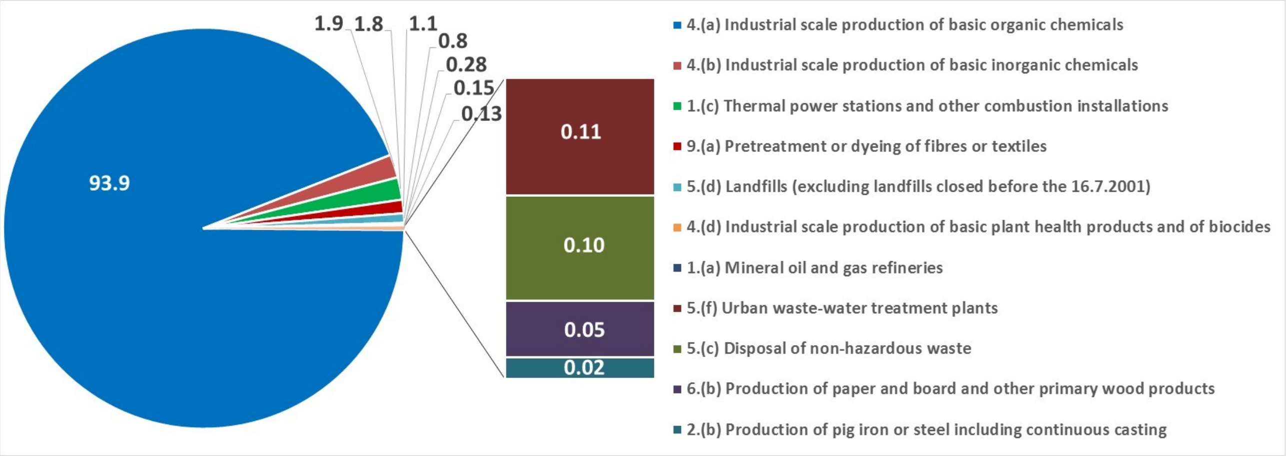

Figure S3. Average percentage contribution of different source sectors to the total CCl_4 emissions reported in the E-PRTR (2007-2014).

Figure S4 shows the average percent contribution to the total CCl_4 flux for each macro area in the EGD over the period 2007-2014. FR alone results to be responsible for 65% of the emissions from the EGD, with an average emission of 0.02 Gg yr^{-1}. Benelux and UK-IE follows with 13.5 and 11%, respectively. NEE, SCA and CH do not report any emission.

As reported in the paper main text (paragraph “Emission hot spots”), the inversion results estimate a CCl_4 emission flux much larger than that declared in the E-PRTR. For major detail, we report in Fig. S5 the percent ratio between emissions reported in the E-PRTR and our estimates for each macro-area in the domain during 2007-2014. The E-PRTR reported emissions from the EGD represent on average, over the considered period, 4 % of the emissions obtained through the inversion. Lower discrepancies are found for the Benelux and FR macro areas where the declared emissions reach the 30 % and 21% of inversion estimation, respectively.

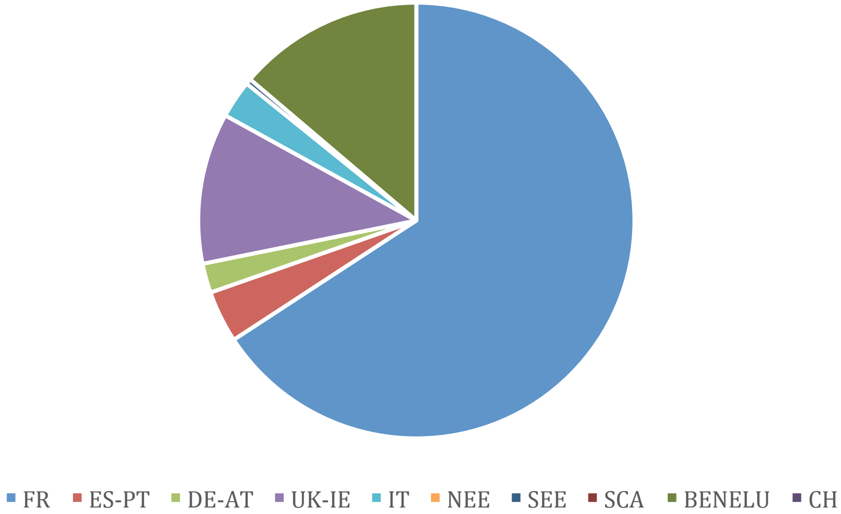

Figure S4. Average percent contribution to the total CCl_4 flux for each macro area in the EGD over the period 2007-2014.

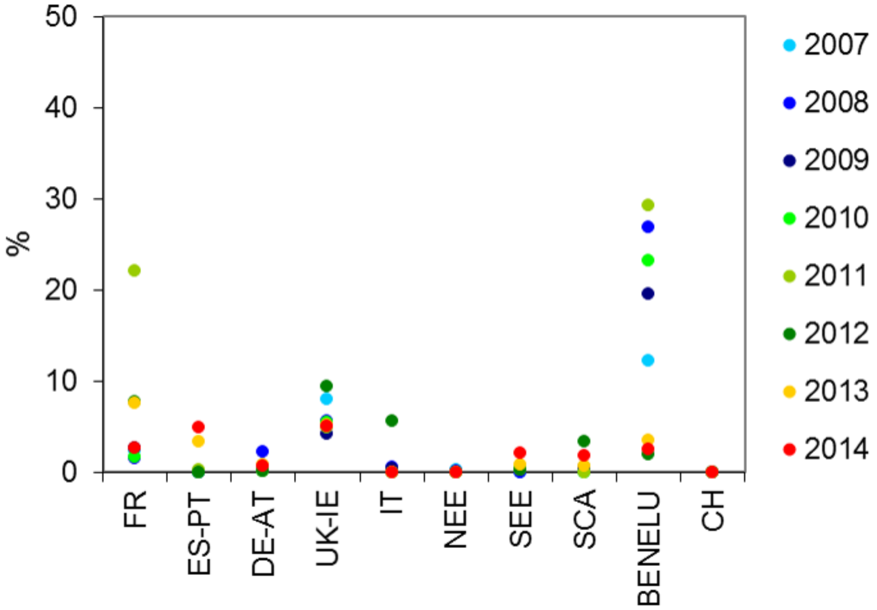

Figure S5. Percent ratio between emissions as in the E-PRTR and the inversion results for each macro-area in the domain during 2007-2014.

Chlorine industry in Europe: Eurochlor

One of the main CCl_4 emission source is the chlor-alkali industry. Information on chlorine and chlorine derivatives production in Europe is given by Eurochlor, an association representing the 97% of chlorine production in Europe. The total number of plants reported by Eurochlor over the period 2006-2014 is 84 (of which 10 in common with the E-PRTR). Eurochlor releases annual reports where potential chlorine production for each industry is given, together with the adopted technology. However, Eurochlor reports do not include information on the CCl_4 emission factors according to the adopted technology. Since 1990's chlorine production in Europe is significantly changed. In 1997 ca 64% of the chlor-alkali industry was based on mercury cell technology and only 10% was based on the cleaner membrane cell process. Currently, the latest accounts by 60% against the 25% of the mercury technology. Over the same period the use of diaphragm cells was reduced from 22 to 12%, while other technologies represent only the 2-3% of the total. Further uncertainties could be due to the employment of CCl_4 in industrial processes where it is used as a process agent in the chlor-alkali plants for the elimination of nitrogen trichloride and the recovery of chlorine from tail gases. In Europe plants that are allowed to use directly CCl_4 (European Union, 2010) were only eight in 2010, of which three in France. However, this source is difficult to assess because the allowed facilities do not have any obligation to report the actual use of the allocated CCl_4 quota and/or the transfer of this quota to another plant. According to DG CLIMA (2012) in 2011 only three chlor-alkali plants in Europe were using CCl_4, and reported emissions ranged from 0 to 30 g CCl_4/tonne annual chlorine capacity, depending on the frequency of use and the occurrence of accidents (Brinkmann et al., 2014).

The graph in Figure S6 reports the percent potential chlorine production for each macro area. The major contributor is the DE-AT macro area accounting for 40%, followed by Benelux with 15.8%. FR, that according to the E-PRTR is responsible for the 65% of European CCl_4 emissions, is the third potential chlorine producer, accounting for the 12%.

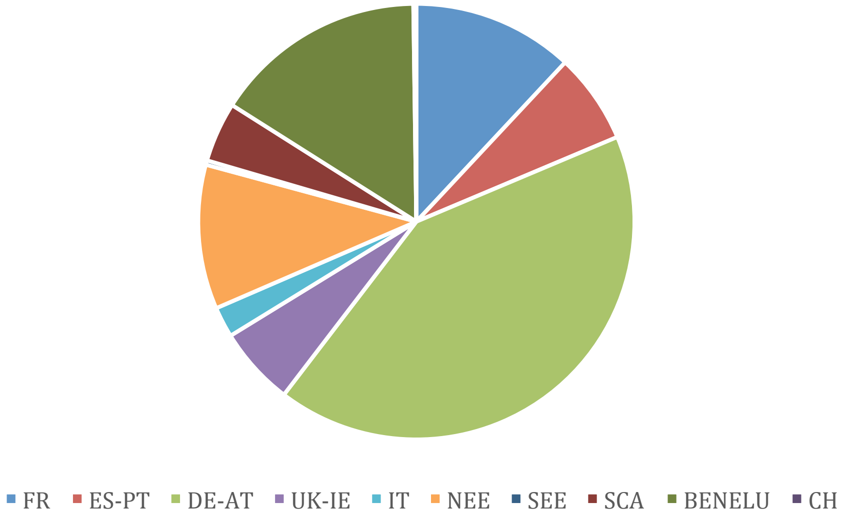

Figure S6. Percent potential chlorine production for each macro area in the EGD (Eurochlor, 2014).

In Figure S7 the percentages of adopted technologies in each macro area in the EGD are reported. It should be noted that in ES-PT, CH and NEE more than 50% of the production is still based on the mercury cell technology. In FR and DE-AT there is still a significant use of diaphragm cells. To be noted that within the DE-AT macro area, Eurochlor does not report any plant in Austria.

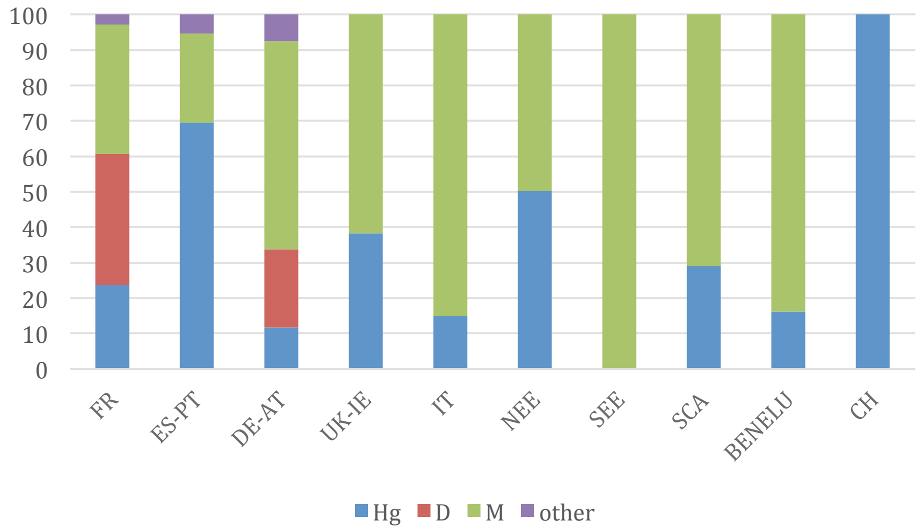

Figure S7. Percentages of adopted technologies in each macro area. Hg: mercury cell technology; D: diaphragm cell; M: membrane cell (Eurochlor, 2014).

A priori emission field

The construction of the *a priori* emission field is a challenging aspect of the methodology adopted in this study, since CCl_4 emission fluxes are affected by high uncertainty.

Possible CCl_4 emission sources are: chlor-alkali plants (UNEP, 2012); emissions produced by feedstock use; petrol-chemical, pesticide, and fire extinguisher industry (UNEP, 2006; 2012); methane chlorination, toxic waste treatment, landfills, incinerators (Fraser et al., 2014); and bleach containing domestic cleaning agents (Odabasi et al., 2008; 2014).

The latest have been evaluated up to 0.49 Gg yr^{-1} for a population of 600 millions in the EGD and this amount has been distributed following the population (CIESIN, 2010) density in all the *a priori* emission fields tested in this work. The remaining non-diffuse emissions have been parameterised following six different ways (F1-F6).

A reference CCl_4 emission value for Europe is that given by Xiao et al. (2010), who estimated an average emission of 3.0 ± 1.6 Gg yr^{-1} over 1996-2004. Since our tests have been performed for the year 2012, we applied to such average value a 2% decrease, following the projection given by Fraser et al. (2012), resulting in an emission from the EGD of 2.38 Gg yr^{-1}.

Here we give a detailed description of each *a priori* emission field tested: Please note that fluxes taken by Eurochlor and E-PRTR are always geo-referenced:

F1: 0.49 Gg yr^{-1} distributed according to the population density; 1.89 Gg yr^{-1} (i.e., the total estimated EGD emission of 2.38 Gg yr^{-1} minus the 0.49 Gg yr^{-1} diffuse emission) are attributed to the chloro-alkali plants evenly distributed among each single plant given in the E-PRTR and in the Eurochlor databases.

F2: 0.49 Gg yr^{-1} distributed according to the population density; 1.89 Gg yr^{-1} as follows: 50% of this flux is evenly distributed among each of the 37 plants listed in the E-PRTR and 50% evenly distributed among the Eurochlor plants (74); in this way F2 assigns a greater role to the E-PRTR plants.

F3: as for F2 but the 50% attributed to the E-PRTR plants is distributed according percent relative contribution to emissions declared by each plant (i.e., if a plant is declaring the 20% of the total CCl_4 reported in the E-PRTR, we assign to this plant the same percentage); similarly, for the Eurochlor plants the 50% is distributed according to the percent relative distribution of the declared chlorine production.

F4: the emissions declared in the E-PRTR, i.e. 0.064 Gg yr^{-1} have been distributed among the single cells where plants are located (Eurochlor plants not included because no information about CCl_4 emissions is given by this database), while 2,32 Gg yr^{-1} (i.e. the total estimated EGD emission of 2.38 Gg yr^{-1} minus the 0.064 Gg yr^{-1} E-PRT flux) are distributed according to the population density.

In addition, we have tested two *a priori* emission fields where the total EGD emission do not correspond to the 2.38 Gg yr^{-1} derived from Xiao et al. (2010):

F5: 0.49 Gg yr^{-1} distributed according to the population density; to such value a flux is added calculated applying an emission factor of 0.4 kg CCl_4 for each tonne of chlorine produced by all plants included in the Eurochlor database. Finally the CCl_4 emissions as declared in the E-PRTR are added. It should be noted that the *a priori* emission flux derived corresponds to 4.4 Gg yr^{-1} for the EGD in 2012. The 0.4 kg CCl_4 for each tonne of chlorine produced emission factor has been suggested by Paul Fraser (personal communication).

F6: as in F5, but applying an emission factor of 0.03 kg CCl_4 for each tonne of chlorine produced by all plants (Brinkmann et al., 2014) included in the Eurochlor database. It should be noted that the *a priori* emission flux derived corresponds to 0.6 Gg yr^{-1} for the EGD in 2012.

In order to evaluate the inversion performance for the various *a priori* emission fields tested, we compared i) the correlation values (ra^2) between the modelled and the observed concentration time obtained using the *a priori* emission fluxes F1÷F6; ii) the correlation values (rb^2) between the modelled and the observed concentration time obtained using the *a posteriori* emission fluxes F1÷F6. In Table S1 the ra^2 and rb^2 values for each station are reported as well as the emission flux produced by a given *a priori* emission field (F1÷F6) from the entire EGD. In all the reported tests, rb^2 values are always higher than ra^2 values, i.e. the *a posteriori* emission field gives account of a better representation of the variance of the measured signal with respect to the *a priori*. In addition, "EGD emission" *a posteriori* values obtained using quite different *a priori* emission fields are very similar (well within the error bar), confirming that the inversion is robust enough and converges towards a reliable emission estimate. In light of such results, we decided to use an "ensemble" *a priori* emission field, built as follows: to each macro area we assigned an emission flux given by the average, for that macro area, of the *a posteriori* emission fields produced by F1÷F6. The share given by diffuse emission has been distributed according to the population density, whereas the remaining share has been equally assigned (and geo-referenced) to each plant in that macro area. The "Ensemble" row in Table S1 reports the ra^2 and rb^2 values, as well as the obtained EGD emission flux. The "Ensemble" *a priori* emission field has been used for estimating CCl_4 emissions over the study period.

Table S1. Comparison among different *a priori* emission fields. F1÷F6 and "Ensemble" represent the *a priori* emission fields described in the text. ra^2: Correlation between modelled concentration fluxes obtained by a given *a priori* emission field and the observations at the three measurement sites. rb^2, as ra^2 but for the *a posteriori* emission fluxes. The tests have been performed for year 2012.

***A priori* emission field**	**CMN**		**JFJ**		**MHD**		**EGD emissions**
	ra^2	rb^2	ra^2	rb^2	ra^2	rb^2	Gg yr^{-1}
F1	0.45	0.58	0.31	0.42	0.66	0.79	2.3 ± 0.8
F2	0.45	0.58	0.29	0.39	0.66	0.79	2.1 ± 0.8
F3	0.40	0.58	0.27	0.37	0.59	0.78	2.2 ± 0.8
F4	0.48	0.58	0.35	0.44	0.70	0.78	2.1 ± 0.7
F5	0.38	0.58	0.25	0.37	0.35	0.78	2.4 ± 0.9
F6	0.49	0.58	0.32	0.42	0.74	0.79	2.1 ± 0.8
Ensemble	0.49	0.58	0.35	0.44	0.75	0.79	2.3 ± 0.8

Subsets of data

Because of the limited numbers and localisation of the receptors, the simulations cannot produce a homogeneous sensitivity over the study domain. In order to assess to what extent our results are sensitive to the receptors used, we run the inversions removing one station at a time

The EGD emissions obtained with different subsets of observation data are consistent with those obtained using the full set. The larger difference, 26 %, is registered when removing MHD. Removing JFJ and CMN, produced a similar percentage difference of -10 % and -9 %, respectively, as a consequence of the similar footprint of the two receptors. This result indicates the stability of the inversion system even when using a subset of data and reinforce the benefit of the increased sensitivity over domain when using an increasing number of receptors.

Model performance at the stations

With the aim of evaluating the model performance and the station specific errors, we compared the observed and modelled time series at the three stations, taking into account different statistical parameters, in a similar way as described in Stohl et al. (2009), Maione et al. (2014) and Graziosi et al. (2015). The results of this comparison, carried out for the year 2012, are reported in Table S2.

$1 - E_b/E_a$ is the relative error reduction, where E_a and E_b are the *a priori* and *a posteriori* RMS errors. The values achieved at the stations used in this study are in a range between 16 % and 23 %, in spite of the different station characteristics.

The Pearson correlation coefficients described in the following show a better performance for MHD because of the poorer model performance in the mountain area. However, as stated in Mahowald et al. (1997), using receptors closer to the main source regions would improve the model performance to acquire source information.

r_a^2 is the squared Pearson correlation coefficients between the time series obtained at receptor using the *a priori* emission field and the observed time series, and r_b^2 between the *a posteriori* and observed time series. These coefficients are used to evaluate the proximity of the modelled emission field to the real one. The obtained r_b^2 values higher than r_a^2 are an indication of the improvement of the *a posteriori* emission field with respect to the *a priori*.

Analogously to r_a^2 and r_b^2, the squared Pearson correlation coefficients r_{ba}^2 (and r_{bb}^2) between the modelled *a priori* (and *a posteriori*) and the measured baseline mixing ratios at the three stations indicate the capability of the system to reproduce the variability and trends of the baseline.

Transport events from the source regions to the receptors generate the variability in the observed enhancements above the baseline. The correlation analyses between the observed and simulated *a priori* (r_{ea}^2) and the *a posteriori* (r_{eb}^2) polluted mixing ratios describe the system capability to reproduce concentrations above the background. Higher correlation values are obtained at the remote station of MHD. Despite the relatively low r_{ea}^2 and r_{eb}^2 values at CMN and JFJ, data from these two mountain stations improve the inversions on the regional scale, thanks to the station sensitivity to the main source regions. For the same reason, the two mountain stations also present higher standard deviation (SD) of the observed mixing ratios.

Table S2. Station parameters. Mean, mean CCl4 mixing ratios; SD, standard deviation of the observed mixing ratios; N, number of observations; E_a, RMS *a priori* error; E_b, RMS *a posteriori* error; $1-E_a/E_b$, relative error reduction; r^2_a and r^2_b, squared Pearson correlation coefficients between the observations and the *a priori* (r^2_a) and *a posteriori* (r^2_b) simulated time series; r^2_{ba} (and r^2_{bb}) is the squared Pearson correlation coefficients between the *a priori* (and *a posteriori*) baseline and the measured concentrations; r^2_{ea} (and r^2_{eb}) is the squared Pearson correlation coefficients between the *a priori* (and *a posteriori*) enhancements above the baseline and the measured concentrations.

Station	Mean (ppt)	SD (ppt)	N	E_a (ppt)	E_b (ppt)	$1-E_b/E_a$	r^2_a	r^2_b	r^2_{ba}	r^2_{bb}	r^2_{ea}	r^2_{eb}
CMN	85.7	1.1	2039	0.82	0.64	0.23	0.48	0.58	0.53	0.55	0.24	0.33
JFJ	84.7	0.8	2124	1.12	0.94	0.16	0.35	0.44	0.24	0.26	0.19	0.22
MHD	84.9	0.3	2833	0.64	0.50	0.23	0.75	0.79	0.75	0.76	0.55	0.63

References

Brinkmann, T., Giner Santonja, G., Schorcht, F., Roudier, S., Delgado Sancho, L.: Industrial Emissions Directive 2010/75/EU, Integrated Pollution Prevention and Control, Science and Policy Reports. Best Available Techniques (BAT). Reference Document for the Production of Chlor-alkali. EC-JRC, Joint Research Centre of the European Commission, Luxembourg: Publications Office of the European Union, 2014.

CIESIN, Center for International Earth Science Information Network (CIESIN): Gridded Population of the World: Future Estimates, Socioeconomic Data and Applications Center (SEDAC), Columbia University, Palisades, NY, USA, 2010. Available at http://sedac.ciesin.columbia.edu/gpw.

EC DG CLIMA (European Commission, Directorate General Climate Action), Report of undertakings on consumption and emissions of controlled substances as process agents under regulation EC/1005/2009, 2012.

European Union, Commission Decision of 18 June 2010 on the use of controlled substances as process agents under Article 8(4) of Regulation (EC) No 1005/2009 of the European Parliament and of the Council, 2010/372/EU, 2010.

Fang X. K., Thompson R. L., Saito T., Yokouchi Y., Kim J., Li S., Kim K. R., Park S., Graziosi F., Stohl, A.: Sulfur hexafluoride (SF6) emissions in East Asia determined by inverse modelling, Atmos. Chem. Phys., 14, 4779-4791, 2014.

Fraser, P., Dunse, B., Manning, A. J., Wang, R., Krummel, P., Steele, P., Porter, L., Allison, C., O'Doherty, S., Simmonds, P., Mühle, J., and Prinn, R.: Australian carbon tetrachloride (CCl4) emissions in a global context, Environ. Chem., 11, 77–88, 2014.

Graziosi, F., Arduini, J., Furlani, F., Giostra, U., Kuijpers, L. J. M., Montzka, S. A., Miller, B. R., O'Doherty, S. J., Stohl, A., Bonasoni, P., and Maione, M.: European emissions of HCFC-22 based on eleven years of high frequency atmospheric measurements and a Bayesian inversion method, Atmos. Environ., 112, 196, 2015.

Keller, C. A., Brunner, D., Henne, S., Vollmer, M. K., O'Doherty, S., and Reimann, S.: Evidence for under-reported western European emissions of the potent greenhouse gas HFC-23, Geophys. Res. Lett., 38, L15808, doi:10.1029/2011gl047976, 2011.

Mahowald, N. M., Prinn, R. G., and Rasch, P. J.: Deducing CCl_3F emissions using an inverse method and chemical transport models with assimilated winds, J. Geophys. Res., 102, 28153–28168, 1997.

Maione M., Graziosi, F., Arduini, J., Furlani, F., Giostra, U., Blake, D.R., Bonasoni, P., Fang, X., Montzka, S.A., O'Doherty, S.J., Reimann, S., Stohl, A., and Vollmer, M.K.: Estimates of European emissions of methyl chloroform using a Bayesian inversion method, Atmos. Chem. and Phys. 14, 9755-9770, doi:10.5194/acp-14-9755-2014, 2014.

Odabasi M.: Halogenated volatile organic compounds from the use of chlorine-bleach containing household products, Environ. Sci. and Technol. 42, 1445-1451, 2008.

Odabasi M., Elbir T., Dumanoglu Y., & Sofuoglu SC.: Halogenated volatile organic compounds in chlorine-bleach-containing household products and implications for their use, Atmos. Environ., 92, 376-383, 2014.

Stohl, A., Hittenberger, M., and Wotawa, G.: Validation of the Lagrangian particle dispersion model FLEXPART against large scale tracer experiment data, Atmos. Environ., 32, 4245–4264, 1998.

Stohl, A., Forster, C., Frank, A., Seibert, P., and Wotawa, G.: The Lagrangian particle dispersion model FLEXPART version 6.2, Atmos. Chem. Phys., 5(9), 2461–2474, 2005.

Stohl, A., Seibert, P., Arduini,J., Eckhardt, S., Fraser, P., Greally, B. R., Lunder, C., Maione, M., Mühle, J., O'Doherty ,S., Prinn, R. G., Reimann, S., Saito, T., Schmidbauer, N., Simmonds, P. G., Vollmer, M. K., Weiss, R. F., and Yokouchi, Y.: An analytical inversion method for determining regional and global emissions of greenhouse gases: Sensitivity studies and application to halocarbons, Atmos. Chem. and Phys. 9, 1597-1620, 2009.

UNEP/CTOC, United Nations Environment Programme/Chemicals Technical Options Committee, 2006. Report of the Chemicals Technical Options Committee (Nairobi, Kenya).

UNEP/TEAP, United Nations Environment Programme/Technology and Economic Assessment Panel, 2012. Report on the Technology and Economic Assessment Panel (Nairobi, Kenya).

Xiao, X., Prinn, R. G., Fraser, P. J., Weiss, R. F., Simmonds, P. G., O'Doherty, S., Miller, B. R., Salameh, P. K., Harth, C. M., Krummel, P. B., Golombek, A., Porter, L. W., Butler, J. H., Elkins, J. W., Dutton, G. S., Hall, B. D., Steele, L. P., Wang, R. H. J., and Cunnold, D. M.: Atmospheric three-dimensional inverse modelling of regional industrial emissions and global oceanic uptake of carbon tetrachloride, Atmos. Chem. Phys., 10, 10421-10434, doi: 10.5194/acp-10-10421-2010, 2010.